UNIVERSITAT POLITÈCNICA DE CATALUNYA BARCELONATECH

Implementing and Testing Optical Transceivers for Fiber Access Network

A Degree Thesis

Submitted to the Faculty of the

Escola Tècnica d'Enginyeria de Telecomunicació de Barcelona

Universitat Politècnica de Catalunya

by

Marc Domingo Ribé

In partial fulfilment

of the requirements for the degree in

TELECOMMUNICATIONS SYSTEMS ENGINEERING

Advisor: Josep Joan Prat Goma

Barcelona, October 2017

Abstract

Optical coherent systems are developing an important role in nowadays telecommunications. Although the price of this systems are high, they seem to be a feasible option in access networks in a near future.

So, the purpose of this project is to study, design and test potential hardware that could be implemented in the future OLT's and ONU's. In this project two cheap transmitters, more precisely, a DFB and a DEML are implemented and tested. Moreover, a simply front-end AM demodulator is designed and tested.

Many experiments have been designed to obtain relevance information of each designed device that validate them as a potential candidate to take part in the future access networks.

Resum

Els sistemes òptics coherent estan desenvolupant un paper molt important en les telecomunicacions actuals. Encara que el preu d'aquests sistemes sigui elevat, sembla ser que poden ser una bona opció per les futures xarxes d'accés.

Aquest projecta proposa estudiar, dissenyar i testejar hardware que pugui ser implementat en futures ONU's i OLT's. Dos transmissors low-cost, més precisament, un DFB i un DEML seran dissenyats, muntats i testejats. A més també, es dissenyarà un demodulador AM senzill.

Diversos experiments han estat dissenyats per tal de comprovar les característiques més rellevants de cada sistema, per tal de veure si poden ser candidats potencials per poder ser part de les futures xarxes d'accés.

Resumen

Los sistemas ópticos coherentes están desarrollando un papel muy importante en las telecomunicaciones actuales. Aunque el precio de estos sistemas sea elevado, parece ser que pueden ser una buena opción de cara a las futuras redes de acceso.

Este proyecto propone estudiar, diseñar i testear hardware que pueda ser implementado en futuras ONU'sy OLT's. Dos trasmisores low-cost, más precisamente, un DFB y un DEML serán diseñados, ensamblados y testeados. Además, se diseñará y testeará un demodulador AM simple.

Diversos experimentos han sido diseñados para comprobar las características más relevantes de cada sistema para ver si pueden ser candidatos potenciales par ales futuras redes de acceso.

Acknowledgements

I want to dedicate this section to the people that has helped me during my final degree thesis. Firstly, I would like to thank my tutor Josep Joan Prat Goma for the knowledge and help that have provided me throughout this time.

Secondly, I would like to thank Victor Polo, who is the person that stayed with me every day since the project started, mentoring me.

Thirdly I want to thank the 3 PhD students: Juan Camilo Velazquez, Jeison Tabares and Saeed Ghasemi who helped me during this project too.

Finally, thank to my parent for the support that they have given me during this period.

Revision history and approval record

Revision	Date	Purpose
0	20/09/2017	Document creation
1	03/10/2017	Document revision

DOCUMENT DISTRIBUTION LIST

Name	e-mail
Marc Domingo Ribé	Marc.domingo@tsc.upc.edu
Josep Joan Prat Goma	jprat@tsc.upc.edu

Written by:		Reviewed and approved by:	
Date	28/09/2017	Date	3/10/2017
Name	Marc Domingo	Name	Josep Joan Prat
Position	Project Author	Position	Project Supervisor

Table of contents

The table of contents must be detailed. Each chapter and main section in the thesis must be listed in the “Table of Contents” and each must be given a page number for the location of a particular text.

Abstract 1
Resum 2
Resumen 3
Acknowledgements 4
Revision history and approval record 5
Table of contents 6
List of Figures 8
List of Tables: 10
1. Introduction 11
1.1. Objective 11
1.2. Work Plan Structure 12
2. State of the art of the technology used or applied in this thesis: 13
2.1. Coherent Systems 13
2.2. Transmitters 14
2.2.1. DFB 14
2.2.1.1. Laser Rate Equation 15
2.2.1.2. Laser Bandwidth Limitations 16
2.2.2. DEML 17
2.2.3. Coherent Optical Receivers 18
2.2.3.1. Idealized Coherent Detector 18
2.2.3.2. Heterodyne Envelope Detection 19
2.2.3.3. Heterodyne Differential Detection of DPSK Signal 20
2.2.3.4. Heterodyne Receiver for CPFSK Signal 21
3. Methodology / project development: 22
3.1. Subsystems 22
3.1.1. DFB Laser 22
3.1.1.1. Introduction 22
3.1.1.2. Design and Considerations 22
3.1.1.3. Assembly 23

3.1.1.4. Set-ups and Results 24
3.1.2. DEML 28
3.1.2.1. Introduction 28
3.1.2.2. Assembly 28
3.1.2.3. Set-ups and Results 29
3.1.3. Envelope Detector 31
3.1.3.1. Introduction 31
3.1.3.2. Design and Assembly 31
3.1.3.3. Set-ups and Results 32
4. Budget 37
5. Conclusions and future development: 38
Bibliography: 39
Glossary 40

List of Figures

Figure 1 13
Figure 2 15
Figure 3 Power-Current Curve 15
Figure 4 Laser Bandwidth 17
Figure 5 Side view of DEML chip structure 17
Figure 6 Coherent Receiver 18
Figure 7 Heterodyne Envelope Detection 19
Figure 8 Encoder 20
Figure 9 DPSK Detector 20
Figure 10 CPFSK Demodulator 21
Figure 11 TO-Can laser 22
Figure 12 Laser Pins 22
,Figure 13 Laser Schematic 23
Figure 14 Laser Assembled 24
Figure 15 Laser Assembled with the protection case 24
Figure 16 Current-Power Curve Set-up 25
Figure 17 Power-Current Curve Results 25
Figure 18 Laser Bandwidth set-up 26
Figure 19 Laser Bandwidth 27
Figure 20 DEML parts 28
Figure 21 DEML Dimensions 28
Figure 22 28
Figure 23 DEML Set-up 29
Figure 24 29
Figure 25 DFB_DEML current power curve 30
Figure 26 EAM_DEML voltage power curve 30
Figure 27 EAM Bandwidth 30
Figure 28 DFB Bandwidth 30
Figure 29 Signal Before and after the envelope detector 31
Figure 30 Envelope Detector Schematic 32
Figure 31 32
Figure 32 Optimum Relation between Base Band Signal and Residual Modulated Signal 33

Figure 33 Envelope Detector Test setup.....35
Figure 34 PRBS 7 at 1,25Gbps 35
Figure 35 Eye Diagram at the laser output.....35
Figure 36 Signal after the PIN.....36
Figure 37 Spectrum of the signal 36
Figure 38 Signal after the envelope detector 36
Figure 39 Eye diagram 36

List of Tables:

Table 1 14
Table 2 Laser Specifications 22
Table 3 26
Table 4 S11 Matching impedances and Return loss 34
Table 5 S22 Matching impedance and Return loss 34

1. Introduction

This work is framed in the European COCONUT (Cost-effective Coherent ultra-dense-WDM-PON for Lambda-To-the user) project. The main scope of the project was to define, study and realization of a new fully scalable optical access network significantly extending the network dimensions in terms of bandwidth utilization, reach and number of accommodated users. To make the COCONUT an attractive product for a mass deployment the research for the design and implementation of cheap coherent systems, yet effective was essential.

This project rises after ending the COCONUT project in way to search, assembly and test potential hardware that can accomplish the low price and good performance to be implemented in the udWDM ONU's and OLT's.

Moreover, the project is centred specially in the study of new kind of transmitters even though we want to develop a simple and cheap front-end asynchronous ASK receiver as the COCONUT was based in Phase Modulation transceivers due to a future study and comparison.

Two kinds of transmitters will be studied:

- TO-CAN DFB manufactured by SUNSTAR. This laser was selected due to its low prices and good performance. However, this transmitter is not ready for coherent transmission due to the fact it has not temperature control. Yet, the constant evolution of TO-CAN encapsulation will permit in a near future the implementation of a temperature control making it a good candidate for future application in coherent transmission.

- Photonic DEML chip manufactured by III-V Labs. This device is composed by a DFB and a EAM sections. The main idea of this device is use the DFB as a light generator and modulate it with the EAM as an external modulation. It enables a better performance that direct modulation Lasers and its reduced size makes its suitable for Small form-factor pluggable transceptor (SFP). Moreover, the combination of the direct modulation laser with the external modulation due to the EAM could permit multi-label modulations. Therefore, the laser output could be used simultaneously as a transmitter source and a local oscillator input for the receiver.

Related to the front-end asynchronous receiver we have decide to implement an envelope detector, due to the fact is a cheap and has simple design in order to have a first idea of its capability's and compare it to the PSK differential demodulator.

1.1. Objective

After the previous introduction of the background and general's ideas of this project we are going to explain more in detail the scopes of this project. We have divided the goals in 3 categories: one for each transmitter and the other for the AM detector.

- DFB Transmitter:
  - Design a noncomplex schematic for laser interface
  - Obtain the maximum Bandwidth of the Laser
  - Enable to modulate the laser from DC

- DEML chip Transmitter:
  - Design a suitable protocol to assembly the DEML into the case specially designed to make the DEML pins accessible.
  - Mount the Set-up to measure the performances of the DEML.
  - Obtain preliminary results of the DEML performances
- AM Detector:
  - Design a simple schematic
  - Obtain preliminary results of the Envelope Detector

1.2. Work Plan Structure

After knowing the requirements and specifications we have to plan a Work Breakdown Structure (WBS).

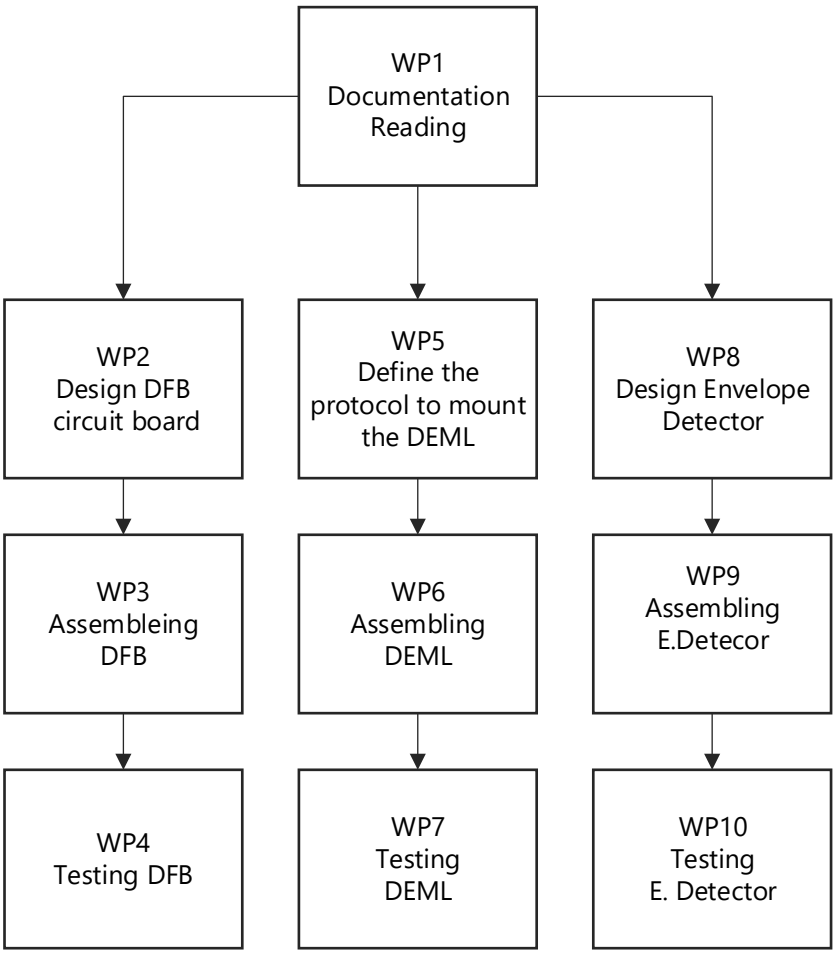

2. State of the art of the technology used or applied in this thesis:

This section is dedicated to introducing basic concepts of coherent systems. Hence, firstly we introduce some basic concepts of the transmitters used in the project, more in particular the tools that permit characterizing the behaviour of the laser. Secondly, we introduce the concepts that permit analyse an ideal coherent receiver; moreover, we introduce some basic schemes of asynchronous coherent receivers.

2.1. Coherent Systems

Despite the rapid progress made in lightwave technology over the past two decades, the basic operations of a digital optical fiber communications link in access networks have reminded essentially the same. They consist in the direct IM (intensity Modulation) of the light source (on-off modulation) and the DD (direct detection) at the receiver site using a PIN or APD (avalanche photodiode).

The huge bandwidth of optical fiber, together with the great improvement of their loss characteristics in the 1970s, led to the success of the simple and reliable IM-DD systems, which, despite their primitiveness and scarce appeal to the sophisticated information theorist, proved to the superior to cable and radio relay systems so as to become the winners for point-to-point high capacity links. However, the increasing demand of bite rate question if a more sophisticated technology will be needed to satisfice this increasing demand.

Ultra-Dense WDM appears as an alternative to increase available bandwidth (BW) by accommodating many users in very narrow channel spacing on a single fiber. The main enabling technology capable to reach these goals inside a UDWDM environment is CO detection.

CO systems present many advantages with respect to the conventional DD systems due to their high selectivity and low sensitivity. Regarding the first one, in a WDM environment with CO detection, channel selection is done after photodetection by sharp electrical filters instead of optical filters. The use of a LO and advanced modulation formats allow to improve the sensitivity and spectral efficiency when compared with DD systems.

In CO systems, the received signal is mixed with a LO laser by means of an optical hybrid or coupler, as seen in Figure 1. The resulting combination is detected by a photodiode(PD) whose output electrical current contains the information carried by the optical field.

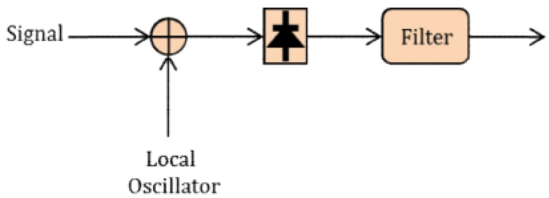

Figure 1

CO systems can be classified in homodyne, heterodyne or intradyne depending on the use of an intermediate frequency (IF) stage. In a homodyne system, the incoming optical signal is downconverted directly to base-band in the photodetection stage, whereas in heterodyne detection it is downconverted into an IF higher than the bit rate. An intradyne system can

be considered either a “near-zero” IF heterodyne system, or homodyne system without phase locking. An electrical spectral diagram comparing coherent systems is provided in Table 1.

System	IF spectrum	IF
Homodyne	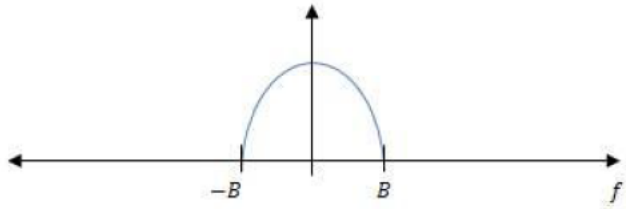	IF = 0
Heterodyne	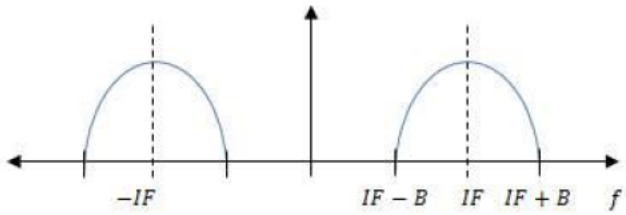	IF > B
Intradyne	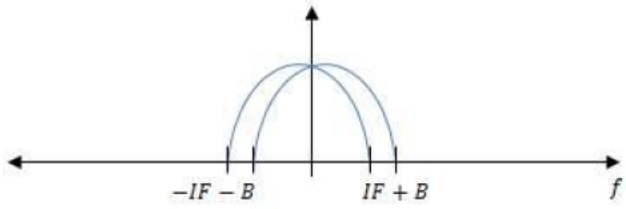	IF < B

Table 1

In heterodyne receivers (Rx) the IF is usually three to five times the base-band signal BW imposing challenges in the BW of the receiver components. [1] An available solution for such an impairment is homodyne detection since it requires only base-band processing. However, such a homodyne Rx needs phase locking between transmitter (Tx) and LO lasers, leading to stringent requirements with the lasers’ linewidth.

2.2. Transmitters

The role of the Optical transmitter is to convert the electrical signal into optical form, and launch the resulting optical signal into the optical fiber. The optical transmitter consists of the following components:

- Optical Source
- Electrical data pulse generator and driver
- Optical modulator (if external modulation)

In this section, we introduce the two transmitters used during this project: the DFB laser, which is used in a wide range of telecommunications applications due to its low cost and good performance, and the DEML, which is and experimental transmitter composed by an DFB and a EAM. Moreover, a brief mention of the main tools used to characterize the lasers in a general way is explained in the DFB part.

2.2.1. DFB

DFB (Distributed feedback Lasers) laser are designed to oscillate in just one longitudinal (and transversal) mode, that is, to produce single frequency light.

In modern DFB lasers a grating is etched onto the entire length of the laser except for a narrow region in the centre whose length is equal to one-quarter the wavelength, $\lambda/4$. These lasers are known as quarter wavelength shifted DFB laser, see Figure 2.

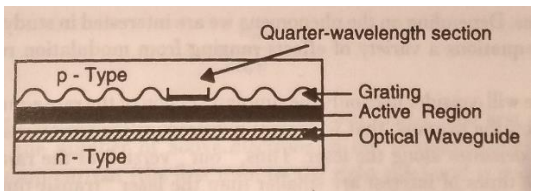

Figure 2

The Power-Current curve is an important characteristic to modelate a laser behaviour. 3 stages can be differensiated:

- **Spontaneous emission stage:** Current injected is below the current thresahold. The photon emited has a random phase and direction in which the photon propagates.
- **Stimulated Linear Emission stage:** Current above the current threshold. The emitted photon mathces the original photon not only in energy, but also in phase and propagation direction.
- **Saturation stage :** Non-linear emssion stage.

Figure 3 show graphicaly the three statges in fucntion of the bias current inject.

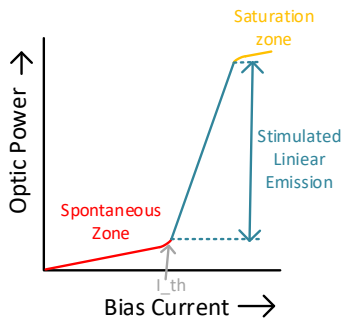

Figure 3 Power-Current Curve

Depending on the modulation used to modulate the DFB, the laser should be biased in the linear stage or near the saturation stage. For example a better performance for ASK modulation is accomplished when the DFB is biased in the middle of the linear stage. However, to have the better perfomance of a PSK or a FSK modulation the laser is biased near the saturation part.

The behaviour of laser can be modelated using the Laser Rate Equations.

2.2.1.1. Laser Rate Equation

Rate equations are powerful analytical tools that provide an understanding of many important properties of semiconductors lasers. We consider here the simplest version of the rate equations which are valid when the time of interest is smaller than the laser “transit time” (Bandwidth of interest smaller than 100GHz).They describe the time variance of the carrier (n) and photons (ϕ) densities:[1]

$$\frac{dn}{dt} = \frac{J}{qd} - \frac{n}{\tau_{sp}} - Cn\phi \left[\frac{1}{m^3 \text{sec}}\right]$$

EQ. 1

$$\frac{d\phi}{dt} = Cn\phi + \delta\frac{n}{\tau_{sp}} - \frac{\phi}{\tau_{ph}} \left[\frac{1}{m^3 sec}\right]$$

EQ. 2

where J is the current density in A/m^2, q is the electron charge, d is the thickness of the recombination region, $\tau_{sp}$is the spontaneous emission lifetime, C is a constant accounting for the strength of stimulated emission, τ_{ph} is the photon lifetime in the laser cavity, and δ is the fraction of spontaneous photons that adds to the lasing mode.

Using the upper rate equations, the operation characteristics of semiconductor lasers are well described. Hence the BW(bandwidth), the RIN (Relative Intensity Noise), the phase and frequency noise and the chirp can be modelled knowing the internal structure design of the laser.

2.2.1.2. Laser Bandwidth Limitations

Depending if an analog or digital transmission systems is used to modulate the laser, there is a way for each system that can determine the maximum bandwidth the laser can achieve.

- **Analog Transmissions**

Analog links are characterized by transmitting continuous-wave (CW) sinusoidal tests signals. In this section, an evaluation of the laser response to a CW sinusoidal excitation in the form denoted in EQ. 3 is considered.

$$J = J_0\left[1 + m_j \exp(j\omega_m t)\right]$$

EQ. 3

Where J_0 is the bias current density, m_j is the current modulation depth and ω_m is the modulation frequency. We have assumed the laser is biased above the threshold.

Using EQ. 3 and the rate equations we obtain a simplified equation of the photon density variation ($\Delta\phi$) due to the modulation. EQ. 4 for $\Delta\phi$ can be broken into three parts:

- The low-frequency (or DC) value, $\Delta\phi(\omega_m = 0)$, which is the same equation as the steady-state situation.
- The frequency dependent term $M(\omega_m)$
- The term $\exp(j\omega_m t)$, reflecting the modulation imposed

$$\Delta\phi(\omega_m) = \Delta\phi(\omega_m = 0)M(\omega_m)\exp(j\omega_m t)$$

EQ. 4

where $M(\omega_m)$ results to have a second -order low-pass form:

$$M(\omega_m) = \frac{1}{1 - \left(\frac{\omega_m}{\omega_0}\right)^2 + j\left(\frac{2\alpha\omega_m}{\omega_0^2}\right)}$$

EQ. 5

And $\Delta\phi(\omega_m = 0)$ is defined by:

$$\Delta\phi(\omega_m = 0) = \frac{1}{Cn_{th}}\frac{m_j J_0}{qd}$$

EQ. 6

where $m_j J_0$ is the current density swing due to modulation.

As can be appreciated in the EQ. 4 the frequency response of a laser is fully defined by the $M(\omega_m)$. The laser bandwidth is limited by the laser resonant frequency, ω_0. Moreover, the bandwidth of the laser is directly affected by the quotient between the laser damping constant and the relaxation oscillation frequency, $\frac{\alpha}{\omega_0}$, as the bandwidth of the laser increase while incrementing this quotient. However, the flatest bandwidth is obtained when $\frac{\alpha}{\omega_0} = 0.7$. (see Figure 4)

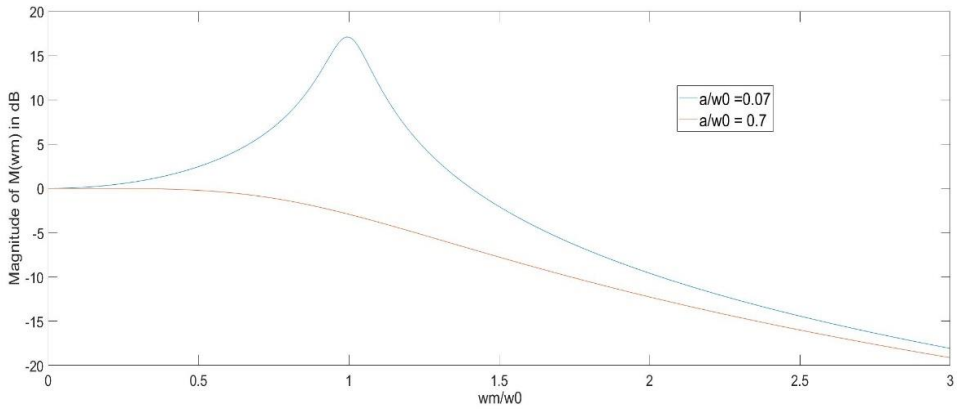

Figure 4 Laser Bandwidth

- **Laser Modulation Step Response**

In digital transmission systems, the information is usually transmitted in the form of binary pulses. The largest bit rate we can achieve is, therefore limited by:

$$R_b \leq \frac{1}{\Delta t_{01} + \Delta t_{10}}$$

Where Δt_{01} is the time required to switch the laser from binary 0 to binary 1, and Δt_{10} is the time required to switch the laser from binary 1 to binary 0.[1]

2.2.2. DEML

A monolithically integrated dual electroabsorption modulated laser (DEML), consiststing of distributed feedback laser (DFB) and electroabsorption modulator (EAM) sections. Figure 5.

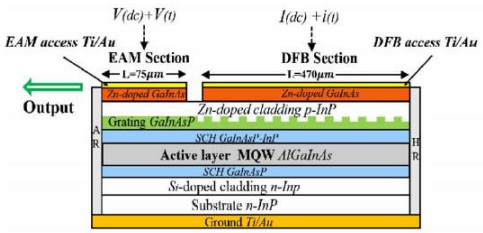

Figure 5 Side view of DEML chip structure

Traditionally, DEML uses the DFB as the optical carrier source and the EAM for data modulation in intensity. Unlike the traditional design on this kind chip, the DFB can be also driven with radio frequency (RF) access, providing capacity of modulating the DFB.

2.2.3. Coherent Optical Receivers

Coherent detection of Optical signal is first used for its superior receiver sensitivity compared to on-off keying. Equivalently speaking, the mixing of receiver signal with the local oscillator (LO) laser functions as an optical amplifier without noise enhancement. Even with the advances of Erbium-doped fiber amplifiers (EDFA), coherent detection can still provide better receiver sensitivity than amplified on-off keying. [3]

In this chapter an idealized receiver for coherent detection is studied. Moreover, we will introduce different structures of real coherent asynchronous receivers based on the modulation used.

2.2.3.1. Idealized Coherent Detector

Figure 6 depicts an idealized receiver for coherent detection. The incoming optical signal is perfectly mixed with the LO and the beting signal is converted to electrical domain by an ideal PD. In the following analysis, it is assumed the case of heterodyne Rx, where optical signals are combined at the desired Intermediate frequency ($\omega_{IF} = \omega_s - \omega_{LO}$) .

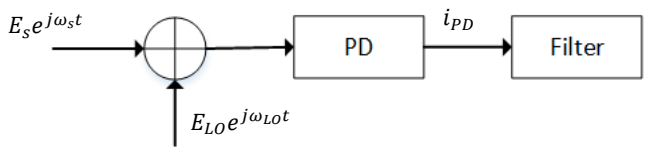

Figure 6 Coherent Receiver

The output current from the PD assumes the form:

$$i_{PD} = R|E|^2 = R\left|E_s e^{j\omega_s t+\phi_s} + E_{LO} e^{j\omega_{Lo} t+\phi_{Lo}}\right|^2$$

$$= R(P_s + P_{Lo} + 2\sqrt{P_s P_{LO}}\cos(\omega_{IF} t + \phi_s - \phi_{lo}))$$

EQ. 7

being R the PD responsivity, P_S and P_{LO} the signal and the LO optical powers respectively. Afterwards our desired signal ($2\sqrt{P_s P_{LO}}\cos(\omega_{IF} t + \phi_s - \phi_{lo})$) is bandpass-filtered to limit the noise before down-conversion and then the decision.

There are mainly two types of noise: shot noise, which is always present because of the quantum-nature of light, and thermal noise, caused by the electronic section of the Rx. Both are white random process. At the filter output, the signal to noise ratio (SNR) can be calculated as:

$$SNR = \frac{\langle i_s^2(t)\rangle}{\langle i_{sh}^2(t)\rangle + \langle i_{th}^2(t)\rangle}$$

EQ. 8

where:

$\langle i_{sh}^2(t)\rangle = qRP_{LO}$ is the shot noise contribution

$\langle i_{th}^2(t)\rangle = 2kT/R_L$ is the thermal noise contribution

By replacing in EQ. 7 it is obtained**:**

$$SNR = \frac{4R^2P_SP_{LO}}{\left(2qRP_{LO} + \frac{4kT}{R_L}\right)B}$$

EQ. 9

Where B is the filter bandwidth. Usually $P_{LO} \gg P_S$ reaching the quantum-limit SNR as:

$$SNR = \frac{2RP_S}{qB} = \frac{2\eta P_s}{B} = \frac{4\eta P_s}{(h\nu)R_b} = 4\overline{N_R}$$

EQ. 10

As it can be appreciated in the upper equation by Controlling the power of the P_{LO}, the shot noise limit can be achieved even for receivers whose performance is generally dominated by thermal noise.

EQ. 10 shows that the quantum-limit SNR is linearly proportional to the optical signal power. However, this linearity depends on having sufficient LO power.

2.2.3.2. Heterodyne Envelope Detection

Figure 7 depicts the scheme of a Binary Heterodyne ASK Envelope detector. Once the signal is converted from optical to electrical the Photodetector, the signal is band-pass filtered (BPF) to limit the amount of noise and then using the envelope detector the signal is squared and low-pass filtered.

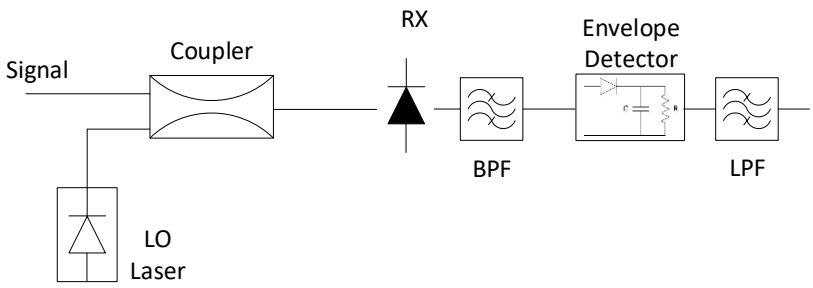

Figure 7 Heterodyne Envelope Detection

The approximated bit error rate (BER) of this receiver is represented for the following equation:

$$p_e \approx \frac{1}{2}\exp\left(-\frac{N_R}{2}\right) \approx \frac{1}{2}\exp(-2 * SNR)$$

EQ. 11

Where $N_R$is the average number of the receiver photons per bit. This bit is related to the incoming optical power by the expression:

$$N_R = \frac{P_S}{(h\nu)R_b}$$

EQ. 12

where P_S is the optical power, ν is the optical frequency and R_b the data bit rate.

Based on EQ. 11 the required SNR for an error probability of 10^{-9} is $N_R = 40$ .The quantum Limit is thus 40 photons/bit.

2.2.3.3. Heterodyne Differential Detection of DPSK Signal

The optical differential BPSK carries data in the phase difference between two consecutive symbols, eluding the need of phase synchronization between TX and LO laser [3]. To avoid error propagation and detect correctly phase changes, it is necessary to encode the transmitted data as depicted Figure 8. The Receiver can employ a simple delay and multiply circuit after PD to find the differential phase Figure 9.

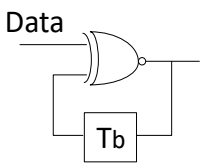

Figure 8 Encoder

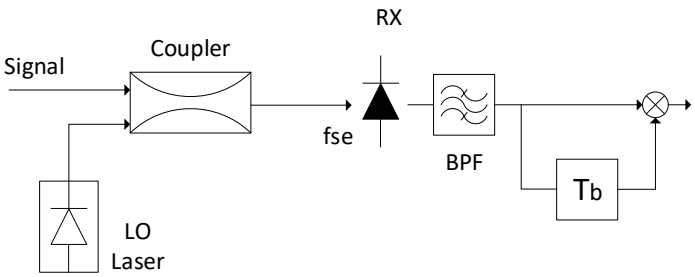

Figure 9 DPSK Detector

For a Binary DPSK modulation, the bit error probability is:

$$p_e = \frac{1}{2}\exp(-N_R)$$

EQ. 13

In this case the required SNR for a bit error probability of 10^{-9} is $N_R = 20$. The quantum limit is 20 photons/bit. We can appreciate that the DBPSK is 3dB better than the ASK. [1]

2.2.3.4. Heterodyne Receiver for CPFSK Signal

The Continuous Phase Frequency Keying (CPFSK) consists in modulate the frequency of the optical carrier in such a way to preserve the continuity of the phase. The CPFSK can be demodulated using the asynchronous receiver the Figure 10 that consists in a differential demodulation with a delay line and a multiplier.

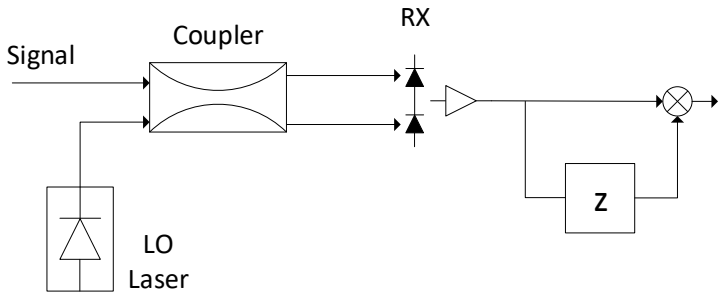

Figure 10 CPFSK Demodulator

The CPFSK with phase continuity can be obtained from the laser output directly, due to the fact that the laser way to modify the frequency is always with a phase continuity.

A particular case of a CPFSK is when the modulation index is 0.5 and de delay $\tau = T_b$. In that case the error probability is the same as the DBPSK mentioned before and its known as Minimum Shift Keying.

3. Methodology / project development:

This chapter explains the methodology used to design and assembly of different hardware and the different set-ups used to calculate basics parameters of that hardware.

3.1. Subsystems

3.1.1. DFB Laser

3.1.1.1. Introduction

The DFB laser used is manufactured by SUNSTAR in simple To-can package. Table 2 Laser Specifications shows the specifications of the laser. Moreover Figure 11 and Figure 12 shows the encapsulation of the laser and its pins distribution.

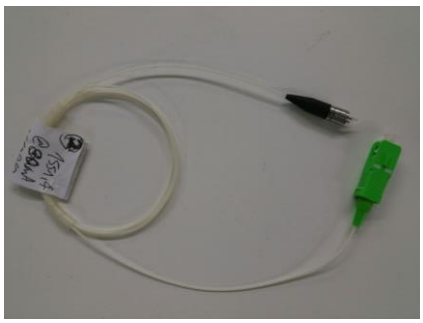

Figure 11 TO-Can laser

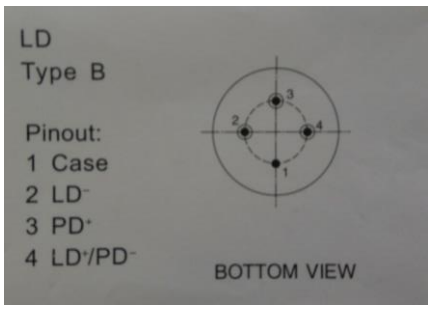

Figure 12 Laser Pins

MODEL	$P_0(mW)$	$I_{th}(mA)$	$E_s(\mu W/mA)$	R_S	λ
SDLP55HAB1SAO	1,51	8,1	77,4	3,8	1550

Table 2 Laser Specifications

3.1.1.2. Design and Considerations

Figure 13 shows the laser schematic; as can be appreciated, the schematic is divided in 3 parts:

- **Bias:** Its function is to inject a specific current to bias the laser to the desired point of operation.
- **RF:** Its function is to modulate the laser property and DC voltage in the RF input.
- **Laser:** It is the element that converts the electrical signal current to optical signal.

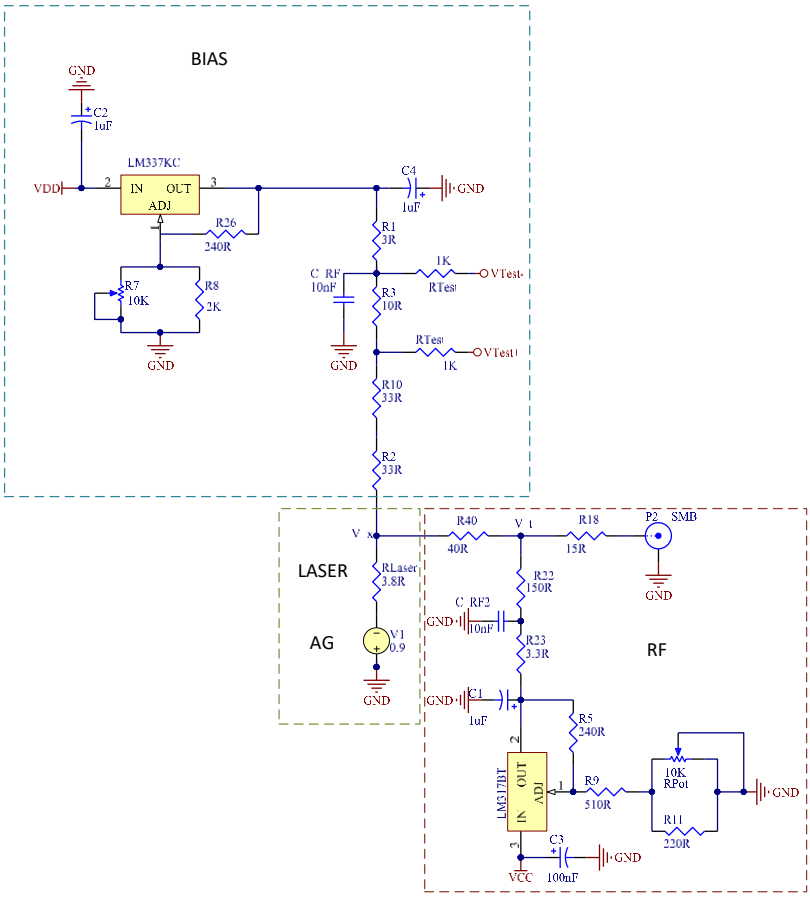

,Figure 13 Laser Schematic

Taking in to consideration the limitations of the laser the maximum current supplied to the laser is 90mA, because the maximum current that the laser can support is around 110mA. Moreover, the DFB is focused on working in the linear part of its Power-Current curve, hence it is not necessary that the laser reaches its maximum saturation state.

Another important consideration was the matching resistance of the circuit. As we have used standard resistance values the perfect theoretical matching of 50Ω is not accomplished, however, we accomplished 48.9Ω.

Moreover, we have introduced a test point in the bias branch that will permit us measure the bias current easying the measure of different parameters of the laser.

We have introduced potentiometers (LM337 and LM317) in the two supply branches to make possible to regulate the laser bias current.

3.1.1.3. Assembly

Due to the fact that the printed circuit board used to assemble the laser was not designed for the laser under test. The following procedures have been followed to assembly the DFB prototypes to accomplish the maximum performance of our transmitter:

1. The laser has to be mounted with the Anode to Ground.
    - The main reason is that the TO-Can contains a photoreceptor too, and because the internal distribution of the TO-Can, it provokes reflections when the laser is mounted with the cathode to ground.

2. The laser case has to be soldered to the ground of the PCB, as it permits a better heat diffusion.
3. Put a RF capacitor at the bias branch and the RF branch.
4. Try to have the shortest RF transmissions lines, since this dielectric presents substantial attenuation at high frequencies.

Figure 14 shows the Laser assembled on the PCB that permit to access to the laser pins. The main parts of the circuit are pointed out.

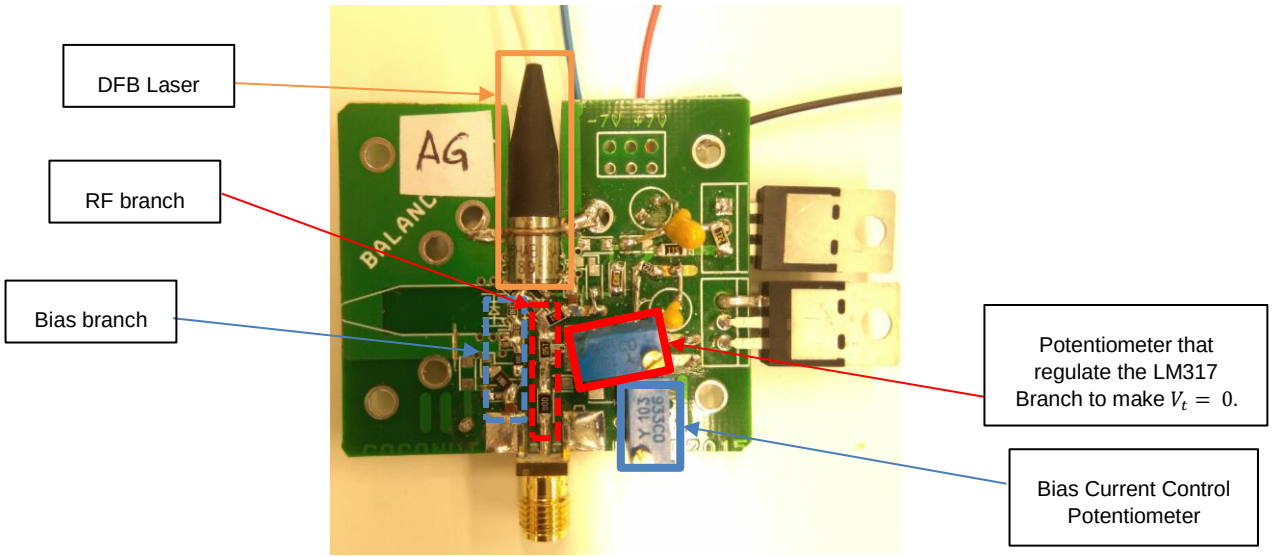

Figure 14 Laser Assembled

To protect the laser, we have mounted a case that allows to interact the laser with a certain protection for the laser. See Figure 15.

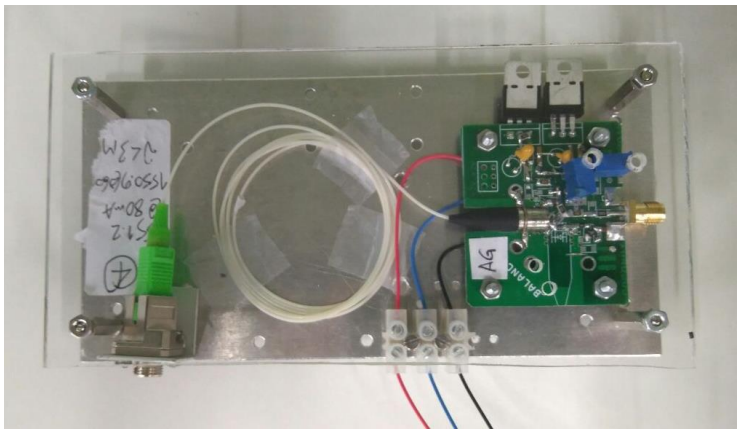

Figure 15 Laser Assembled with the protection case

3.1.1.4. Set-ups and Results

In this subsection the different set-ups used to characterize the laser are described. Explaining the parameters of the laser characterized using the described set-up. The nomenclature that relate, the different parts and components of the laser are shown in Figure 13.

1. Current-Power Curve

Figure 16 shows the set up used to measure the current power curve. With this setup a wide range of electrical parameters of the laser can be deduced.

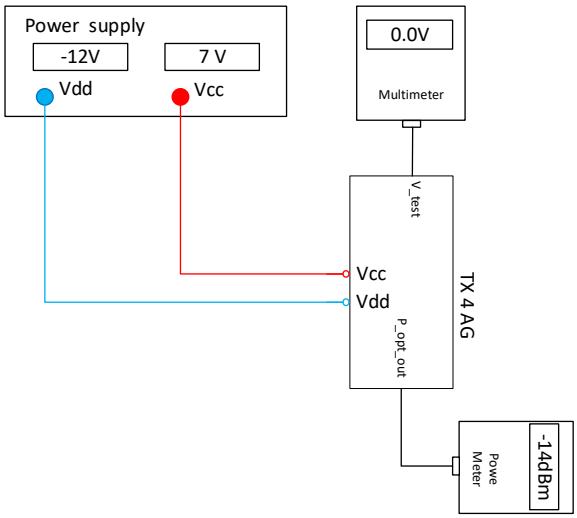

Figure 16 Current-Power Curve Set-up

The procedure we have followed to obtain the desired data was:

1. Inject current to the supply branch by regulating the potentiometer of the LM337.
2. Make V_t = 0 by regulating the LM317.
3. Measure the $\frac{V_{test}}{10}$, it gives the supplied current
4. Measure the Optical Power emitted with a power meter.
5. Measure V_x

With the steps 1-4 we can represent the power curve of the laser. Moreover, with the step 5 we can characterize the equivalent resistance of the laser.

Taking into consideration that the current measured in the supply branch is not the current that biases the laser, if not, the real bias current of the laser is the following:

$$|I_{laser}| = |I_{test}| - |I_{LM317}|$$

The results obtained from this set-up are:

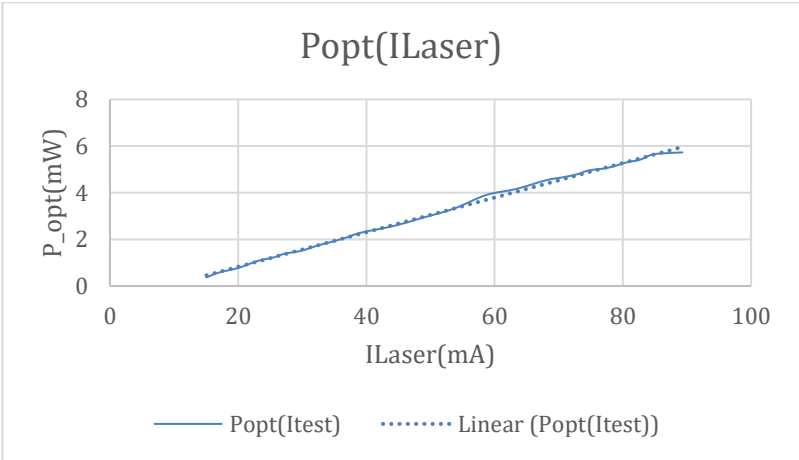

Figure 17 Power-Current Curve Results

Figure 17 shows the Current-power curve; as it can be appreciated the threshold of this laser is around 14mA and it start to saturate at 84mA. From this plot, we can extract the efficiency of our laser, which is 0.0741mW/mA; in this case we have considered the liner part of the graphic.

Moreover, as the laser diode can be modelled as a resistance in series and voltage source we have calculated the real values of them. Table 3 compare the values, given by the manufacturer, used to modulate the electrical behaviour of the laser and the real ones obtained.

	Manufacturer	Real
$R(\Omega)$	3,8	5
$\lvert Voltage\ Source \rvert\ (V)$	0.9	0.825

Table 3

2. Laser Bandwidth

Figure 18 shows the set-up used to measure the bandwidth of the laser. This measure will permit us knowing the maximum bit rate that the laser could achieve with a duobinary ASK.

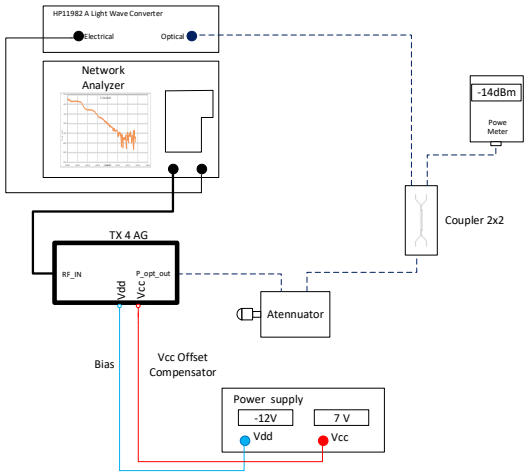

Figure 18 Laser Bandwidth set-up

To get an appropriate result in this set-up many considerations have to be done:

- An attenuator and a Power Meter have to be used to regulate the input power of the optical to electrical converter. As a high-power input could saturated the laser, provoking an undesirable result.
- The Network Analyzer compute the $10log\left(\frac{I_{0ut^2}}{I_{in}^2}\right)$. However, because of the nature of the signal in this case is $10log(\frac{I_{0ut}}{I_{in}})$. Hence, a post processing to the results must be done to show the real bandwidth of the laser.

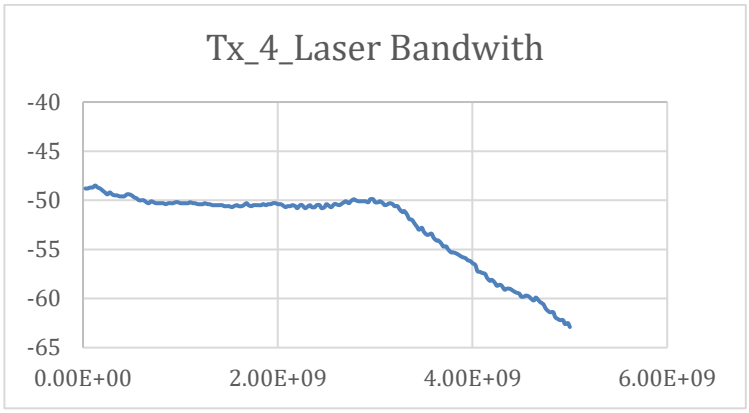

Figure 19 Laser Bandwidth

Figure 19 shows the laser bandwidth when the laser is biased at 55mA. As can be appreciated the $Bw(-1dB) = 3{,}4GHz$, and $Bw(-3dB) = 3{,}7Ghz$

3.1.2. DEML

3.1.2.1. Introduction

The DEML used is made by III-V Labs, a France company. The parts and the dimensions of the chip submount are specified in Figure 20 and Figure 21.

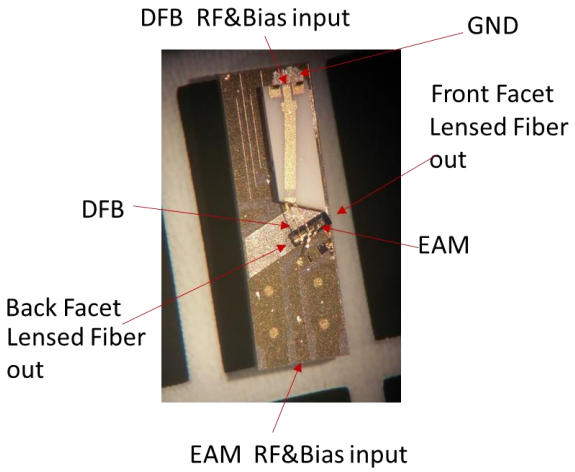

Figure 20 DEML parts

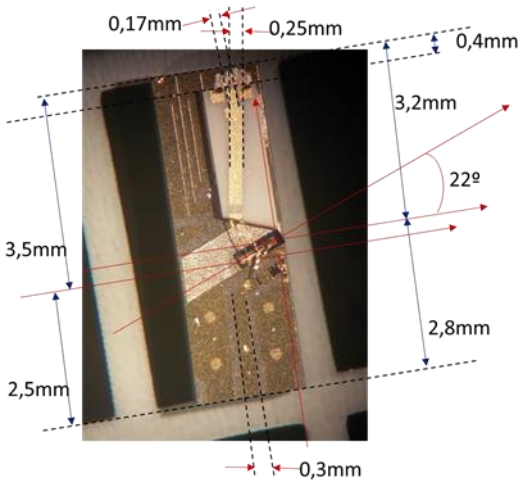

Figure 21 DEML Dimensions

As appreciated in the upper figure, the chip is divided in different parts:

- **DFB RF&Bias input**: Branch that supply the laser to bias it. Moreover, this branch it is used to modulate the laser if necessary.
- **EAM RF&Bias input**: Branch that supply the EAM to bias it and to modulate the EAM if necessary.
- **Front Facet**: This Is the facet where the combination of the DFB and the EAM will emit most of the power.
- **Back Facet:** This Is the facet where the combination of the DFB and the EAM will emit residual power.

3.1.2.2. Assembly

Figure 22 shows the DEML assembled to the respective parts that provide access to the DEML pins. The parts of the final mount can be divided:

- DEML submount: Chip undertest
- NTC(Negative Temperature Coefficient): It is a thermistor that will provide us the temperature of the chip.
- PCB: 50Ω microstrip Teflon substrate.
- SMA RF connectors
- Copper Case:

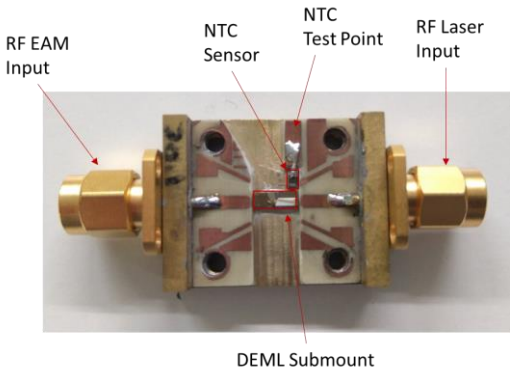

Figure 22

A precise protocol has been designed to assemble all the upper parts to not damage the device undertest, after several tries.

3.1.2.3. Set-ups and Results

Figure 23 shows the set-up used to characterize the current-power curve of the laser and the voltage-power curve of the EAM. Due to the fact there is no an attached fiber to the DEML an ad-hoc solution to guide the output light of the DEML to the measurement device was necessary.

Moreover, as shown in Figure 23 a Peltier is used to maintain the temperature of the DEML constant. As mentioned before an NTC was incorporated near the submount, it is used to monitoring the temperature of the DEML and with that information the Peltier can rectified if a variation of temperature is occurred.

To avoid damage the DEML by light reflections an isolator was fused with the fiber.

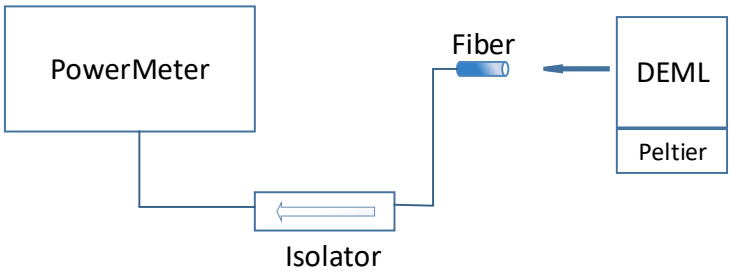

Figure 23 DEML Set-up

Figure 24 shows the set-up used to align the fiber with the DEML. As can be appreciated the fiber is mounted to a 3-axis stage as a millimetric precision is needed to align the fiber. To have the best alignment an angle < 8 degree respect the submount edge totally orthogonal to the submount must to be achieved.

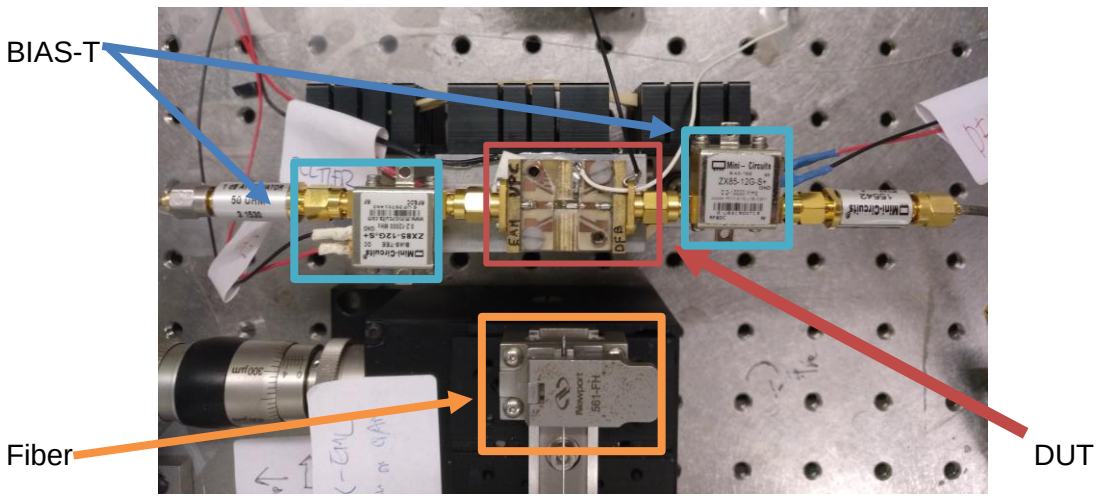

Figure 24

Moreover a maximum transmission power between transmitter and the fiber will be achived when the distance among both is around $50\mu m$.

To characterize the current-power curve of the laser, the EAM was switched off and we increased the bias current of the laser from 0mA to 100mA without modulation at 24ºc. Figure 25 shows the power-current curve of the two DEML mounted. The threshold of boths lasers are around 7 mA and they star to saturate around 94mA.

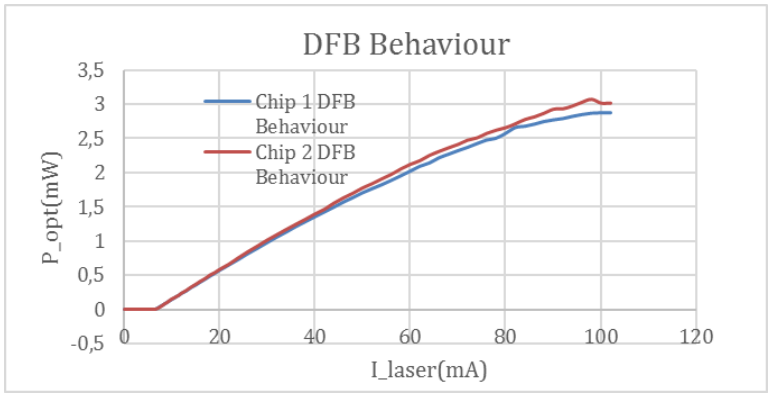

Figure 25 DFB_DEML current power curve

Figure 26 shows the voltage-power curve of the EAM at 50mA bias of the DFB and at 24ºC. To do so, the EAM was biased from 0V to -5V.

From this curve, be can deduce the maximum extinction ratio at 50mA bias laser for an ASK modulation.

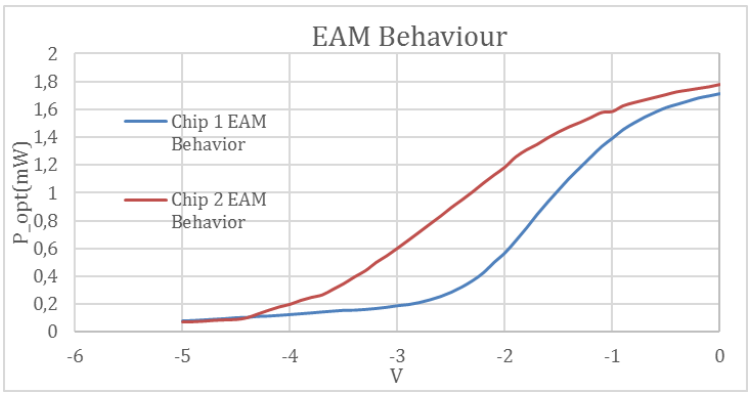

Figure 26 EAM_DEML voltage power curve

Figure 27 and Figure 28 show the EAM and the DFB Bandwidth. Whereas the EAM can reach more than 10Ghz, the DFB reaches around 8GHz.

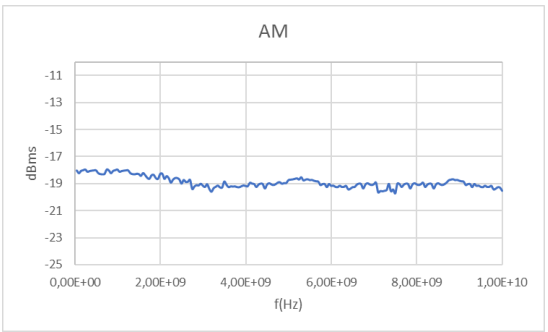

Figure 27 EAM Bandwidth Chip 1

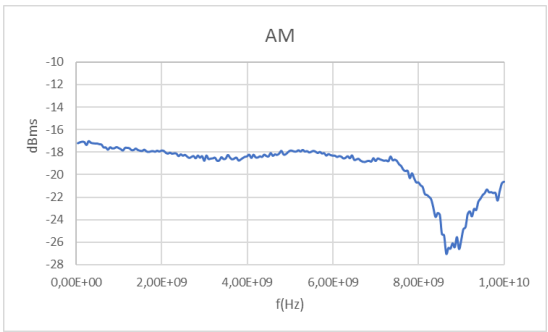

Figure 28 DFB Bandwidth Chip 1

3.1.3. Envelope Detector

3.1.3.1. Introduction

Figure 7 shows an heterodyne asynchronous ask demodulator using an envelope detector. Before talking about the design of the envelope detector we will explain the main concept behind it.

In a heterodyne coherent detection when the transmitted signal is mixed with local oscillator and after the photodetector the signal is downconverter to an IF obtaining the photocurrent of the EQ. 7. After that, the signal can be filtered, eliminating the continuous terms of the signal. However, a down-conversion to base-band is required.

The envelope detector performs this down conversion by its square law response. The EQ. 14 shows the current signal after the envelope detector.

$$i = A^2 cos^2(\omega_{if} t) = \frac{A}{2} + \frac{A}{2}\cos(2\omega_{if} t)$$

EQ. 14

Where:

$A = R * 2\sqrt{P_{LO} P_S}$

As can be appreciate in EQ. 14 two terms can be distinguished, the base-band signal , $\left(\frac{A}{2}\right)$, and the same signal at $2\omega_{if}$, which cannot interfere the base band signal as it is far enough, However, a filter after the envelope detector is required to avoid noise and the residual signal at ω_{if}, as the envelope detector does not perform an ideal square law, Figure 29.

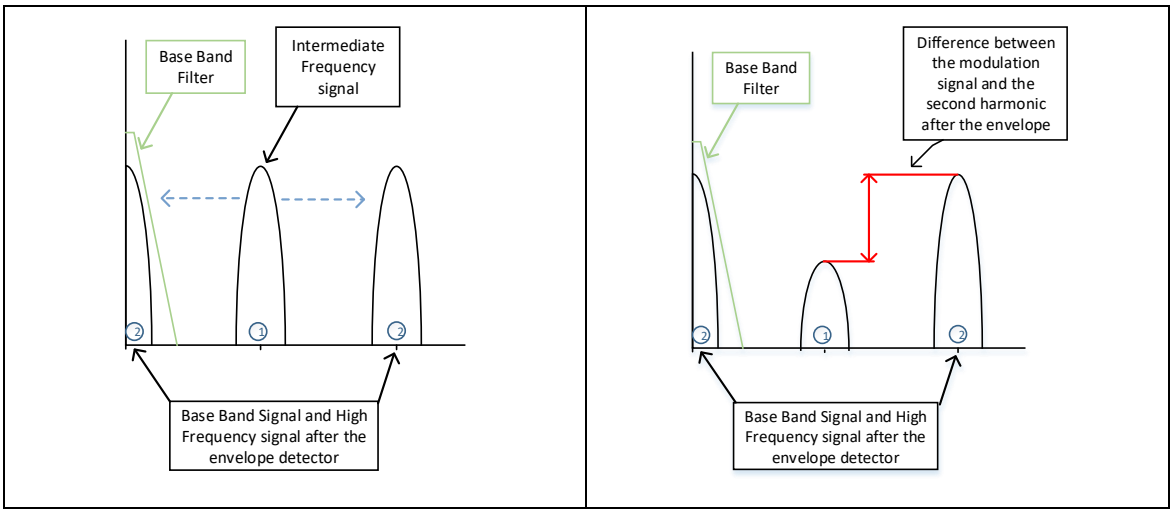

Figure 29 Signal Before and after the envelope detector

3.1.3.2. Design and Assembly

Figure 30 shows the schematic of the envelope detector. A zero bias Schottky diode, more precisely an HSMS 286Y, was selected as it has a wider dynamic range, better thermal stability and more accurate square law response than point contact diode.

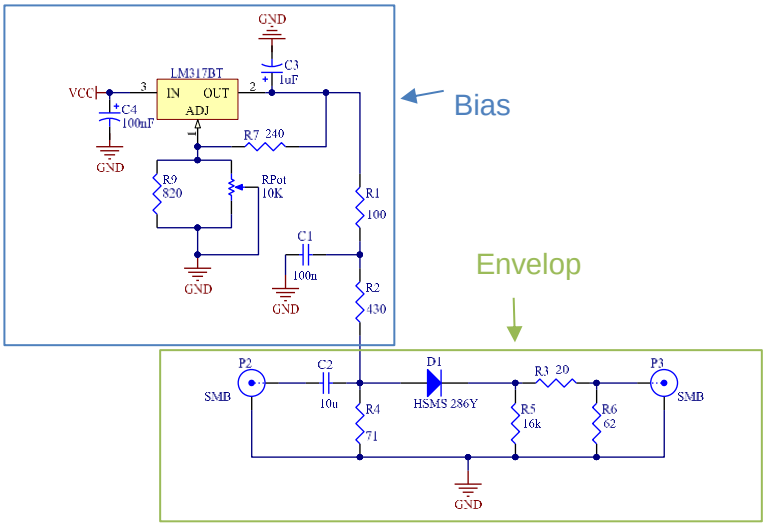

Figure 30 Envelope Detector Schematic

Moreover, two differential parts can be distinguished: the envelope detector and the bias branch, that permit us bias the diode and define the work-point.

3.1.3.3. Set-ups and Results

In this subsection are described the different set-ups used to characterize the envelope detector.

1- Optimum Bias Voltage:

Figure 31 shows the set-up used to define the optimum bias voltage point. To do so, we have defined the following conditions:

- Modulated frequency (f_{mod}) : $10KHz$
- Carrier frequency (f_c): $100KHz$
- Signal Modulation Voltage: $0{,}5Vpp$; $1Vpp$; $2Vpp$

Figure 31

For each signal modulation voltage, we have incremented the bias voltage of the diode from 0 to 5V.

Using the FFT function of the oscilloscope we search for the best relation between the base band signal and the residual modulated signal. Figure 32 shows that the best relation is when $VBias = 2{,}75V$, where we have the maximum of the base band signal and the minimum of the residual modulated signal.

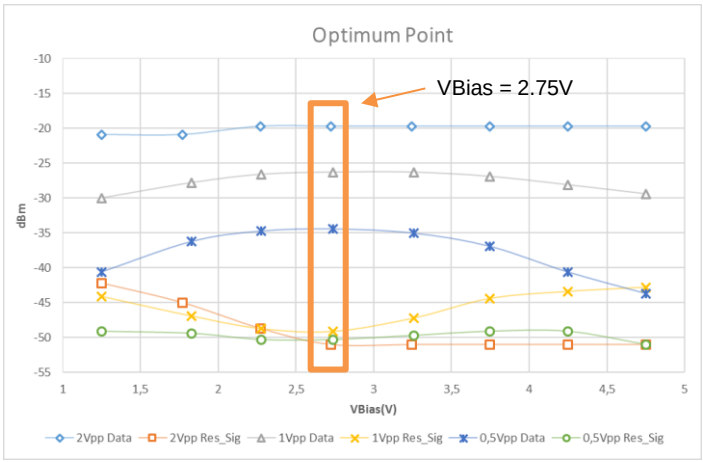

Figure 32 Optimum Relation between Base Band Signal and Residual Modulated Signal

2- Matching

Once defined the optimum point of bias we have measured the matching impedance of the envelope detector with de NA at the input(S_{11}) and at the output(S_{22}) of the envelope detector. Two situations are considered:

1. The matching impedance without bias or $Vbias = 0V$.
2. The matching impedance at optimum bias point, $Vbias = 2{,}75$

Table 4 and Table 5 shows that S_{22} is better adapted than S_{11}.However both are better adapted when Vbias is 2,75V.

S_{11}	
$\boldsymbol{Vbias = 0V}$	$Vbias = 2{,}75V$
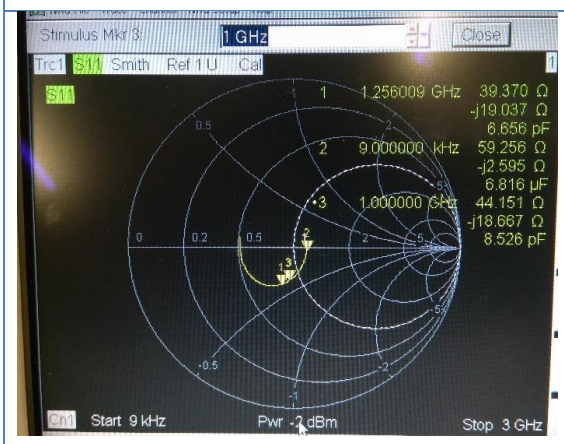	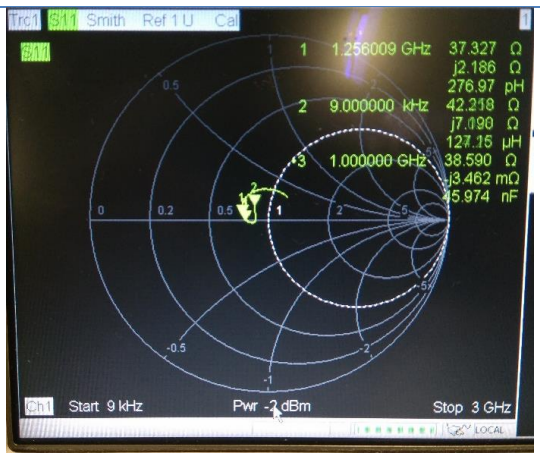

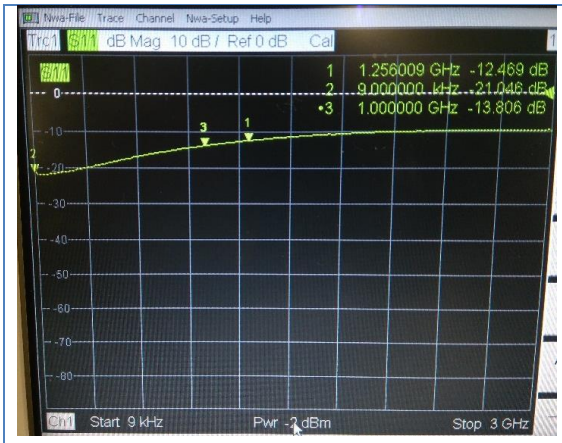

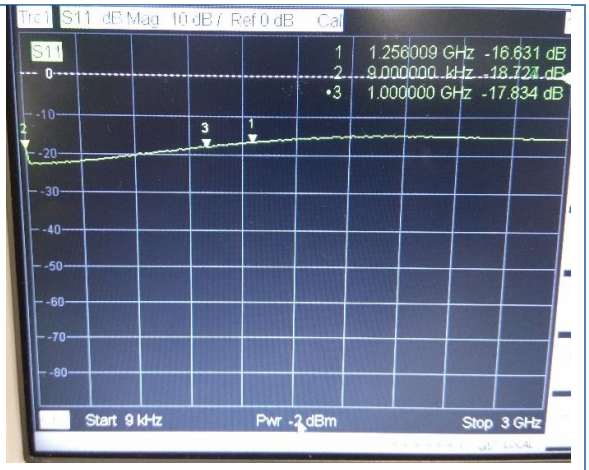

Table 4 S11 Matching impedances and Return loss

S_{22}	
$\boldsymbol{Vbias = 0V}$	$Vbias = 2{,}75V$
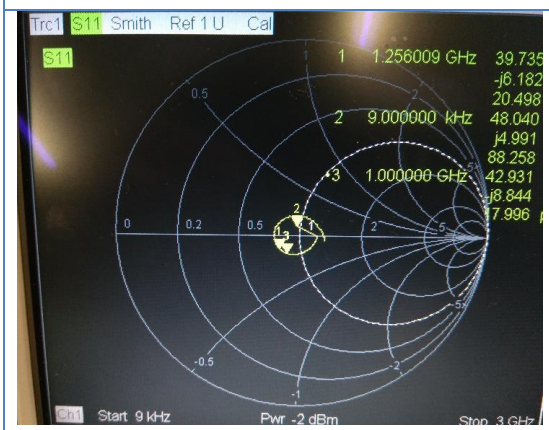	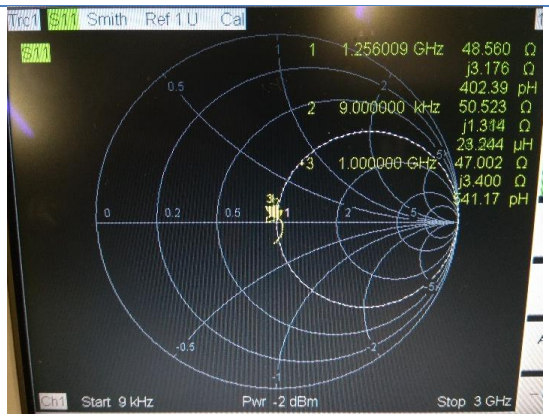
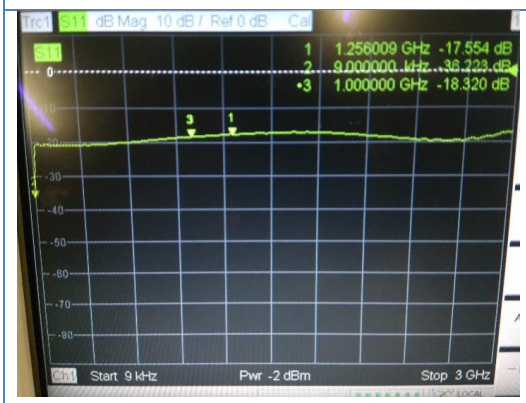	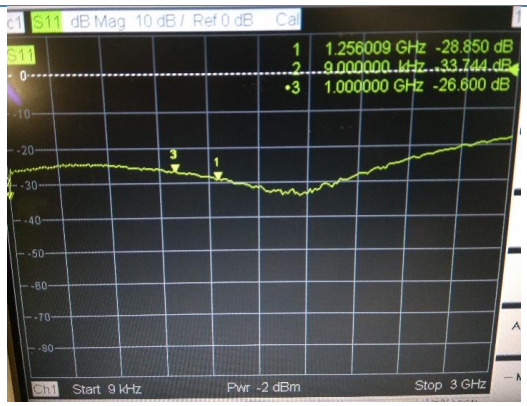

Table 5 S22 Matching impedance and Return loss

3- Qualitative test of the demodulator

To verify that the envelope detector works as expected we have design the setup showed in Figure 33.

An FPGA generate a PRBS 7 at 1,25Gbps to modulate a laser, after that the signal is attenuated, simulating a fiber connection, then the signal is mixed with the local oscillator

and detected by two photoreceptors, one that goes to the envelope detector and after that to the oscilloscope to see the eye diagram of the signal and the other photoreceptor sends signal to the ESA to localize where our signal is placed.

The function of high pass filter used before the envelope detector is to eliminate the base band signal, because the signal of interest is situated at 2,5GHz after mixing our signal with the local oscillator. Then we obtain a signal distribution like Figure 29 and we only want to preserve the base band signal.

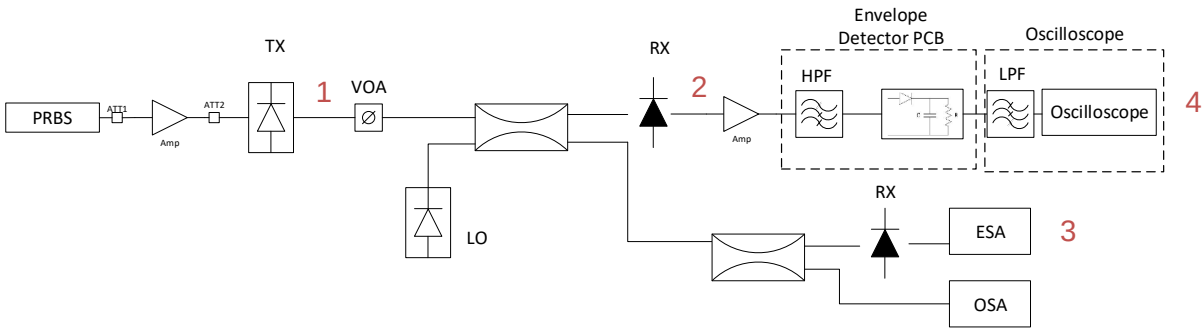

Figure 33 Envelope Detector Test setup

We have analysed the signal in 4 points of the set up:

1. Figure 34 shows the PRBS sequence used to modulate the laser at 1,25Gbps and Figure 35 shows the eye diagram at the laser output.

Figure 34 PRBS 7 at 1,25Gbps

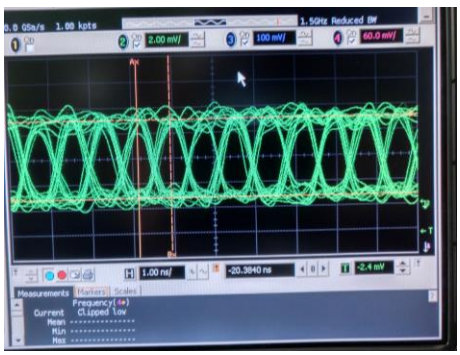

Figure 35 Eye Diagram at the laser output

2&3. Figure 36 the signal after the PIN in time domain. Figure 37 shows the spectrum of our signal, where 2 pics can be appreciatet that is because the laser is a frequency modulator and when you modulate it the “1” are placed in a diferent freqency than the “0”.Hence, to recive a correct signal we must place one of the two pics centered between 2,5GHz and 3,2GHz as the envelope detector bandwith is bellow 4GHz.

Figure 36 Signal after the PIN

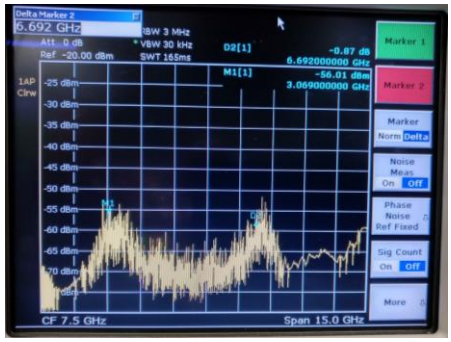

Figure 37 Spectrum of the signal

4. Figure 38 shows the signal detected after the envelope detector in purple and the original signal in green. Figure 39 shows the eye diagram received.

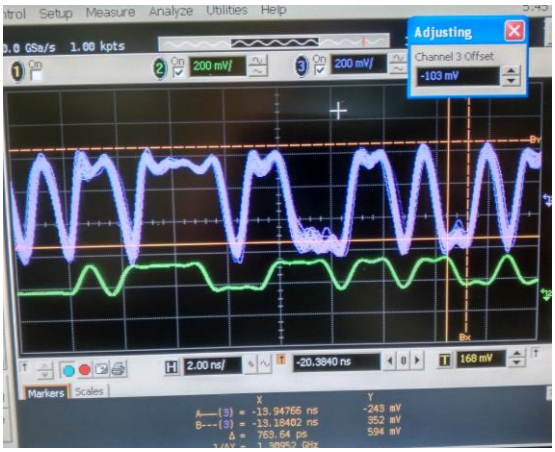

Figure 38 Signal after the envelope detector

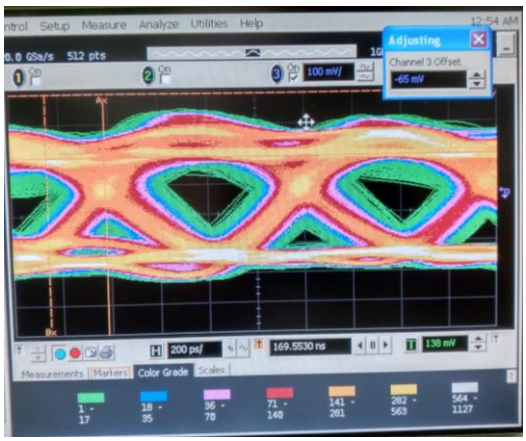

Figure 39 Eye diagram

The upper results are obtained without optimizing the whole set up, although we have obtained the best results as we put the signal to demodulate at 3GHz and we work at 2,75V envelope detector's bias. Moreover, the signal power was -20dBs before mixing it with the local oscillator, which is a relative high power for coherent receiver.

4. Budget

In this chapter the total cost of the studies performed in this work is estimated. We have divided the total cost in 3 stages, one for each implemented device. We take in consideration that a junior engineer salary rounds the 15€/h. Moreover, we only take in consideration the material used to mount the different devices as the equipment necessary to assemble and test is already in the laboratory. The PCB's used are cheap because are made of glass fiber and only have two layers. Although, the PCBs used in this project are reused the cost of this kind of PCBs rounds 10€ per 10 equal PCBs.

Another important thing is that the DEML Chip is not in the market. The DEML used was delivered from III-Vlabs for research.

1. DFB Laser

DFB Laser	50€
Electronics components	<5€
PCB	1€
Junior engineer's wage	2000€

2. DEML Laser

DEML Chip	free
Electronics components	<5€
PCB	1€
Junior engineer's wage	1500€

3. Envelope Detector

Electronics components	<5€
PCB	1€
Junior engineer's wage	2500€

5. Conclusions and future development:

This final chapter concludes the work by exposing the main conclusions. The project has 3 differentiated parts; one for each designed device so we expose the conclusions of each device separately. Yet, before a brief reminder of the general scope of the project is done.

This project consists in design, implement and test different potential devices, more precisely, two transmitters and one AM demodulator, that can accomplish a good performance in spite of their low prices.

Firstly, the electronic part to access the laser interfaces was designed looking for simplicity and trying to achieve the maximum bandwidth as possible and starting it from DC. Although the laser is not suitable for coherent systems as it has not a temperature control. The results prove that our design is good enough that can permit us to modulate the laser from DC to 3,75GHz. Moreover, we have a first design to work with in case the manufacturer of the DFB used launches a new DFB with temperature control.

Secondly, we work in the assembly of two DEML and the design of a suitable set-up to measure their performances. In this case we characterized the current-power curve of the DFB and the voltage-power curve of the EAM, however we only measure the bandwidth of the first DEML. Nevertheless, they are good candidates to be implemented in future commercial transceivers due to the fact its small size and large bandwidth.

Thirdly, a simply and cheap AM demodulator was implemented. The main scope here was to prove the concept of the envelope detector. Although, we prove that our detector is able to demodulate a PRBS 7 at 1,25Gbps signal, our experiments was aiming to get qualitative and not quantitative results.

Finally, the three points defined in this conclusion can have a future development. For example:

- the DFB laser has not an optimized PCB design, because we reused a PCB used in the COCOUNT project, so the performance of the DFB can be improved if we design an optimized PCB for the laser.
- we have characterized the DEMLs, however we do no try to modulate them, so another good point will be to know the behaviour of the DEML for different kinds of modulation.
- The envelope detector could be improved as can be seen in the results the matching impedance of it is not good enough. Moreover, the performances of the envelope detector in terms of BER could be an interesting result, that could be used to compare with another kind of receptors.

Bibliography:

[1] Kazovsky, L., Benedetto, S. and Willner, A. (1996). *Optical fiber communication systems*. Boston: Artech House.

[2] Ramaswami, R., Sivarajan, K. and Sasaki, G. (2010). *Optical networks*. Amsterdam: Elsevier/Morgan Kaufmann.

[3] Ho, K. (2006). *Phase-Modulated Optical Communication Systems*. Dordrecht: Springer.

[4] Prat, J., Angelou, M., Kazmierski, C., Pous, R., Presi, M., Rafel, A., … Ciaramella, E. (2013). Towards ultra-dense wavelength-to-the-user: The approach of the COCONUT project. In *International Conference on Transparent Optical Networks*. http://doi.org/10.1109/ICTON.2013.6602824

[5] Fan, X., Pei, X., & Xiong, X. (2011). Zero bias Schottky diodes use in high performance detection circuits. In *ICEOE 2011 - 2011 International Conference on Electronics and Optoelectronics, Proceedings* (Vol. 3). http://doi.org/10.1109/ICEOE.2011.6013291

[6] Cano, I. N., Lerín, A., Polo, V., & Prat, J. (2014). Direct phase modulation DFBs for cost-effective ONU transmitter in udWDM PONs. *IEEE Photonics Technology Letters*, *26*(10), 973–975. http://doi.org/10.1109/LPT.2014.2309852

[7] Polo, V., Borotau, P., Lerin, A., & Prat, J. (2014). DFB laser reallocation by thermal wavelength control for statistical udWDM in PONs. In *European Conference on Optical Communication, ECOC*. http://doi.org/10.1109/ECOC.2014.6964080

[8] Tabares, J., Polo, V., Cano, I., & Prat, J. (2015). Automatic λ-control with offset compensation in DFB intradyne receiver for udWDM-PON. *IEEE Photonics Technology Letters*, *27*(4), 443–446. http://doi.org/10.1109/LPT.2014.2377095

[9] Sato, K., Kuwahara, S., & Miyamoto, Y. (2005). Chirp characteristics of 40-Gb/s directly modulated distributed-feedback laser diodes. *Journal of Lightwave Technology*, *23*(11), 3790–3797. http://doi.org/10.1109/JLT.2005.857753

[10] research". *In Proceedings of the Fourth International Symposium on Information Processing in Sensor Networks, IPSN 2005*, 25-27 April 2005, Los Angeles, USA. pp. 364-369. doi: 10.1109/IPSN.2005.1440950.

Glossary

AM: Amplitude Modulation

CW: Continuous-Wave

DEML: Dual Electroabsorption Modulated Laser

DD: Direct Detection

DFB: Distributed Feedback Laser

EAM: Electroabsorption Modulator

EDFA: Erbium Doped Fiber Amplifier

ESA: Electrical Spectrum Analyzer

FFT: Fast Fourier Transform

FSK: Frequency Shift Keying

IM: Intensity Modulation

NA: Network Analyzer

OSA: Optical Spectrum Analyser

PCB: Printed Circuit Board

PRBS: Pseudorandom binary sequence

PSK: Phase Shift Keying

SFP: Small Form-Factor Pluggable